A Density Functional Theory Study of Structure, Stability and Reactivity of Clathrate Hydrates

A report submitted towards the partial fulfillment of Five year BS-MS Dual Degree Programme

by

Rohit Kumar

Supervisor: Dr. Arun Venkatnathan

IISER PUNE

Department of Chemistry

Indian Institute of Science Education and Research

Pune

Certificate

This is to certify that this dissertation entitled **"A Density Functional Theory study of structure, stability and reactivity of Clathrate hydrates"** towards the fulfillment of the BS-MS dual degree programme at Indian Institute of Science Education and Research, Pune represents original research carried out by **"Rohit Kumar** at **IISER Pune"** under the supervision of **"Dr. Arun Venkatnathan, Assistant Professor, Chemistry"** during the academic year 2011-2012.

Supervisor:

Date:

Place:

Head Phys/Chem/Bio/Math Sciences

Date:

Place:

Declaration

I hereby declare that the matter embodied in the report entitled **"A Density Functional Theory study of structure, stability and reactivity of Clathrate hydrates"** are the results of the investigations carried out by me at the Department of Chemistry**,** IISER Pune done under the supervision of Dr. Arun Venkatnathan and the same has not been submitted elsewhere for any other degree.

Rohit Kumar

(20071011)

Acknowledgement

Foremost, I would like to express my sincere and heartfelt thanks to my advisor Dr. Arun Venkatnathan whose guidance, incredible support and encouragement always made me feel enthusiastic throughout my project work and enable me to present the work in this thesis.

It is a great pleasure to express my warm and very-very sincere thanks to my fellow lab mate K. R. Ramya for her valuable advice, insightful comments, and discussions. I would like to thank all my fellow lab mates Anurag, Mandar, Minal, Wilbee, Prema, Mubina, for their encouragement and making the lab environment full of enthusiasm. I also want to acknowledge my classmates Shadab, Danveer, Rahul, Piyush, Mohit, Darshan, Anuj, and Vibham for making this period full of joy.

I would like to thank Dr. Anirban Hazra, Dr. Arnab Mukherjee, and Dr. Prasenjit Ghosh for many discussions in our group meeting from which I learnt a lot.

I would like to thank DST for INSPIRE Fellowship and IISER Pune for computing facilities.

Finally I would like to express special thanks to my family for their unconditional support throughout my career and always inspiring me to be successful.

Dedicated to my parents

Table of Contents

List of Figures

List of Tables

Abstract

Clathrate hydrates are formed via the process of nucleation where different gas molecules are encapsulated in water cages. The characterization of stability and reactivity of the clathrate hydrates plays a prominent role in the understanding of nucleation and growth of hydrates. In the present work we employed Density functional theory (DFT) using the M05-2X functional to characterize the structure, interaction energies and reactivity associated with varying occupancy of diatomic gases (H_2, N_2, O_2) in dodecahedron (5^{12}), tetrakaidecahedron ($5^{12}6^2$) and hexakaidecahedron ($5^{12}6^4$) cages. The interaction energies and the reactivity descriptors show that an optimum increase in the occupancy of the guest molecules enhances the stability of the cages. A triple occupancy of H_2, double occupancy of O_2 and N_2 molecules show maximum stability in the 5^{12} cage. A triple occupancy of H_2 and O_2, and single occupancy of N_2 show maximum stability in the $5^{12}6^2$ cage. A quadruple occupancy of H_2, double occupancy of O_2 and triple occupancy of N_2 shows maximum stability in the $5^{12}6^4$ cage.

Keywords: Clathrate hydrates**,** Density Functional Theory, structure, Interaction energy, reactivity descriptors.

1. Introduction

1.1. Clathrate hydrates:

Clathrate hydrates are cage structures made of water molecules in which different gas molecules can be trapped. Clathrate hydrates are crystalline compounds and are found in abundance in the ocean floor[1-6]. These hydrates are formed when water and gas molecules react at low temperature and high pressure[1-2]. During the reaction, water molecules crystallize into a network of hydrogen-bonded cages in which gas molecules (e.g., methane) are trapped. For example, the amount of methane which can be stored in hydrates can be seen from the following example. Each volume of hydrate can contain 184 volume of methane gas at STP[2]. Based on present energy requirements, methane gas hydrates could provide energy for the entire world for the next 200 years[3]**.** While methane gas hydrates are studied widely[1-6], gases like Ar, Kr, O_2, N_2, CO and other hydrocarbons which can be accommodated inside the cages have received attention recently[7].In general, clathrate hydrates can be classified based on structure as described in the next section.

1.2. Crystallographic Structures:

The structures of clathrate hydrates are determined from X-ray crystal diffraction data[2] and are classified into three types. They are sI, sII and sH hydrates. In 1965, McMullan and co-workers[8] described the cages of the hydrates based on fundamental mathematical parameters: The authors described the cages as (N_i^{Mi}), where M_i denotes the number of faces with N_i number of edges. The crystal hydrate structures are composed of various types of water cages. The naturally occurring water cages found in the three structures are as follows: The dodecahedron (5^{12}) water cage consists of 20 water molecules which consist of 12 pentagonal faces and 30 edges (i.e. N_i=5, M_i=12). The irregular distorted dodecahedron ($4^3 5^6 6^3$) water cage consists of 20 water molecules. The tetrakaidecahedron ($5^{12}6^2$) water cage consists of 24 water molecules which have 12 pentagonal faces and 2 hexagonal faces. The hexakaidecahedral ($5^{12}6^4$) water cage consists of 28 water molecules which consist of 12 pentagonal faces and 4 hexagonal faces. The icosahedron water cage ($5^{12}6^8$) consists of 36 water molecules which consist of 12 pentagonal faces and 8 hexagonal faces. The structures of some water cages are shown in Fig.1.The crystallographic parameters for different clathrate hydrate structures are shown in Table 1. The sI hydrate is formed by interconnected two 5^{12}

cages and six $5^{12}6^2$ cages. The sII hydrate is formed by interconnected sixteen 5^{12} cages and eight $5^{12}6^4$ cages. Similarly, sH hydrate is formed by interconnected three 5^{12} cages, two $4^35^66^3$ cages and one $5^{12}6^8$ cage.

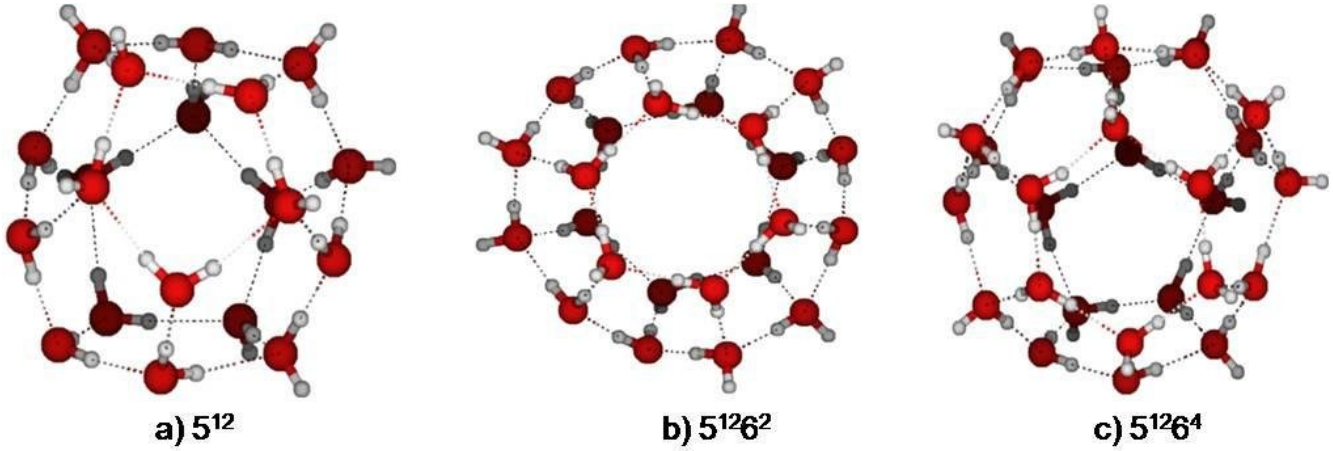

Figure 1: Cages of the sI and sII hydrate lattice.

Table 1: Crystallographic parameters for clathrate hydrate structures[9]

Hydrate crystal structure	sI		sII		sH		
Cavity	Small	Large	Small	Large	Small	Medium	Large
Description	5^{12}	$5^{12}6^2$	5^{12}	$5^{12}6^4$	5^{12}	$4^35^66^3$	$5^{12}6^8$
Number of cavities per unit cell	2	6	16	8	3	2	1
Average cavity radius(A^0)	3.95	4.33	3.91	4.73	3.91	4.06	5.71
Coordination number	20	24	20	28	20	20	36
Number of water per unit cell	46		136		34		

1.3. Brief description of previously reported work:

Experimental studies have shown the phase transformation, thermo-dynamic stability and spectral properties of clathrate hydrates. Qiang *et al*.[14] studied the phase transformation of methane hydrates under high pressure. The authors observed at T= 323 K and P= 880 Mpa, the sI hydrates transforms to form sH hydrate. However at T = 348 K and P = 960 Mpa, sH hydrate decomposes to form methane and water. Sloan and co-workers[15] recorded the Raman spectra of gas molecules like CH_4, CO_2 and their mixtures in different cages of the hydrate lattice. The authors suggested that Raman spectra can be employed to observe the formation of these hydrates. Sloan and coworkers[16] also showed the occupancy of the guest molecules in different water cages obtained from the sea floor was in good agreement with measurements from the laboratory synthesized natural hydrates.

It is well known that varying guest molecules can be encapsulated inside these hydrates depending upon the size of the guest and the radius of cavity of the cages of the hydrates. Further, the encapsulation of guest molecules is also dependent on the nature of guest[10.] For example, hydrophobic non polar guest molecules can be trapped at temperature < 300 K and pressure 0.6 Mpa in suitable cages[3]. For polar guest molecules, encapsulation occurs below 100 K and at pressure below 0.133 Mpa[10].Computational methods like Molecular Dynamics (MD) simulations and quantum mechanical methods have been employed to understand the stability of clathrate hydrates. Roger[11-12]and co-workers performed MD simulations to study the nucleation of methane gas hydrates from a methane/water system. The authors described the hydrate nucleation mechanism using a “labile cluster hypothesis” and a “local structuring hypothesis”. The authors performed MD simulations at different temperatures to observe the formation of the cages. However, the authors could not observe the complete crystallization process since the simulation time was confined to a few nanoseconds. Hawtin *et al*.[13] employed MD simulations on a methane/water interface system and observed a spontaneous nucleation. The authors concluded that nucleation proceeds via a formation of a tetrahedral network of water molecules that resembles a 5^{12} cage. Horikawa *et al.*[17]employed MD simulations to characterize the dynamic behavior of N_2 and O_2 molecules in the cages of the sII clathrate hydrate. The authors observed that the doubly occupied N_2 and O_2 in the $5^{12}6^4$ cages were stable whereas the single occupancy of the N_2 and O_2 gases in the 5^{12} cages were stable. van Klaveren *et al.*[18] employed MD simulations to study the stability of doubly occupied N_2 in

sII clathrate hydrates. The authors found at varying temperature and pressure, the doubly occupied N_2 clathrate showed maximum stability. Alavi *et al.*[19] employed MD simulations to study the stability of sII H_2 clathrate hydrates using varying occupancies. The authors concluded that configurations with a single H_2 occupancy in the 5^{12} cages and quadruple H_2 occupancy in the $5^{12}6^4$ cages were found to be the most stable.

Complementary to MD simulations, there are some *ab initio* calculations on the stability of encapsulation of gases on the explicit cages. Tse *et al.*[20] used the Density Functional Theory (DFT) with a B3LYP functional and showed that the 5^{12} cages showed maximum stability with double occupancy of H_2 which contradicts the MD simulations results of Alavi. However, the authors found that the $5^{12}6^4$ cages show stability with quadruple occupancy of H_2 which was consistent with the observations of Alavi.[19] Chattaraj *et al.*[21] investigated the encapsulation of H_2 using DFT and B3LYP functional. The authors concluded that both the 5^{12} and $5^{12}6^2$ cages attain maximum stability when it accommodates two H_2 molecules. Sathyamurthy and co-workers[7] employed the MP2 method to characterize the single occupancy of host-guest interactions present only in the 5^{12} cages. The authors observed that the single occupancy of N_2 shows maximum stability compared to the single occupancy of O_2 and H_2. Sastri and co-workers[22] investigated the occupancy of CO_2 inside various cages of s-I, s-II, and s-H hydrate lattice. The authors concluded that among all cages, the CO_2 uptake for the 5^{12} cage was the least favorable.

1.4. Scope of the project:

This work employs a Density Functional Theory with a M05-2X[23] exchange correlation functional to characterize the binding of varying guest molecules in 5^{12}, $5^{12}6^2$ and $5^{12}6^4$ cages. Such a study serves as an important tool for understanding clathrate hydrates that can capture and store various gases of importance to energy and environment.

1.5. Aim of the presented work:

The objective of this study is to understand the binding and reactivity of, diatomic guest molecules like H_2, N_2, and O_2 encapsulated in various cages (5^{12}, $5^{12}6^2$, and $5^{12}6^4$) of the clathrate hydrates.

2. Method:

2.1. Theoretical Background:

The quantum mechanical approach to find the solution of the time independent and non-relativistic Schrodinger equation is defined[24] as:

$$\hat{H}\psi_i = E_i\psi_i \tag{1}$$

ψ_i is the wave function for any chemical system in its i[th] state. E_i gives the energy of the system in the i[th] state. $\hat{H}$ is the Hamiltonian operator for any system which consists of M nuclei and N electrons:

$$\hat{H} = -\frac{1}{2}\sum_{i=1}^{N}\nabla_i^2 - \frac{1}{2}\sum_{A=1}^{M}\frac{1}{M_A}\nabla_A^2 - \sum_{i=1}^{N}\sum_{A=1}^{M}\frac{Z_A}{r_{iA}} + \sum_{i=1}^{N}\sum_{j>i}^{N}\frac{1}{r_{ij}} + \sum_{A=1}^{M}\sum_{B>A}^{M}\frac{Z_A Z_B}{R_{AB}} \tag{2}$$

The first and second terms represents the kinetic energy of the electrons and nuclei respectively, third term represents the electron-nuclei attraction, fourth and fifth terms represents the electron-electron and nuclei-nuclei repulsion respectively. Since the mass of the nuclei is heavier than the mass of the electrons, the nuclei are assumed to be fixed in space, where electrons can move in the field generated by the nuclei. Thus, the nuclear kinetic energy term is neglected and the nuclei-nuclei repulsion term is kept as constant. This is known as the Born-Oppenheimer approximation[24]. The resultant Hamiltonian can be written as follows:

$$\hat{H}_{elec} = -\frac{1}{2}\sum_{i=1}^{N}\nabla_i^2 - \sum_{i=1}^{N}\sum_{A=1}^{M}\frac{Z_A}{r_{iA}} + \sum_{i=1}^{N}\sum_{j>i}^{N}\frac{1}{r_{ij}} \tag{3}$$

$$\hat{H} = \hat{T} + \hat{V}_{Ne} + \hat{V}_{ee} \tag{4}$$

$\hat{H}_{elec}$ is known as electronic Hamiltonian and $\hat{V}_{Ne}$ is the attractive potential. This is also called as an external potential ($\hat{V}_{ext}$) in Density Functional Theory. The Schrödinger equation can now be written as:

$$\hat{H}_{elec}\psi_{elec} = E_{elec}\psi_{elec} \tag{5}$$

where,

$$E_{total} = E_{elec} + E_{nucl} \tag{6}$$

While methods like Density Functional Theory, Configuration interaction, Coupled Cluster methods, Moller-Plesset perturbation theory, can be employed to study many electron systems, we focus our attention only on Density Functional Theory due to the computational

ability to study large molecular systems like clathrate hydrates[25]. In the next section, a brief description of Density Functional Theory is provided.

2.2. Density Functional Theory:

Density functional theory (DFT) was initially developed by Walter Kohn and co-workers[26-27]. Conceptually, DFT mirrors traditional *ab initio* methods, where the electron density $n(r)$, plays a key role. The beginning point of the DFT is the Hohenberg and Kohn (HK) first theorem[26] which states that "The specification of the ground state density $n(\vec{r})$, determines the external potential v_{ext} or $v(\vec{r})$ uniquely (to within an additive constant)."

$$n(\vec{r}) \rightarrow v(\vec{r}) \text{ (Unique)} \tag{7}$$

N (Number of electrons) can be determined from n(r) by integration.

HK second theorem[26] states that the functional $F_{HK}[n]$ delivers the ground state energy of the system. This energy will be the lowest if the input density is the true ground state density (n_0). The energy functional is sufficient to determine the ground state energy and the density and is written as:

$$F[n(r)] = \langle \psi | \hat{T} + \hat{V}_{ee} | \psi \rangle \tag{8}$$

We can write an equation in terms of charge density as follows:

$$E_V[n(r)] = F[n(r)] + \int n(r)v(r)dr \tag{9}$$

and $$E_{v(r)}[n(r)] \geq E_{v(r)}[n_0(r)] = E_0 \text{ (ground state energy)} \tag{10}$$

The largest and elementary contribution of the $F[n(r)]$ can be seen as follows[26-27]:

$$F[n(r)] = T_S[n(r)] + \frac{1}{2}\int \frac{n(r)n(r')}{|r-r'|} drdr' + E_{xc}[n(r)] \tag{11}$$

In eqn.11, $T_s[n(r)]$ gives the kinetic energy of a non-interacting system which has a density $n(r)$. The second term is the classical expression of the interaction energy. The last term (E_{xc}) is the exchange correlation energy. The Euler-Lagrange equation associated with

$E_v[n(r)]$ can be transformed into Kohn-Sham (KS) equations (self consistent) which are described below[27]:

$$(-\frac{1}{2}\nabla^2 + v(r) + \int \frac{n(r')}{|r-r'|}dr' + v_{xc}(r) - \varepsilon_j)\varphi_j(r) = 0 \quad (12)$$

$$n(r) = \sum_{j=1}^{N} |\varphi_j(r)|^2 \quad (13)$$

$$v_{xc}(r) = \frac{\partial E_{xc}[n(r)]}{\partial n(r)} \quad (14)$$

Here v_{xc} is exchange correlation potential. All the equations written above can be solved using a self-consistent approach. The determination of v_{xc} in each cycle is from an approximation for $E_{xc}[n(r)]$ which will be described further. The KS equations are (in principle) exact, if an appropriate E_{xc} can be determined. Hence, any source of error arise only due to the choice of E_{xc}. The ground state energy can be written as follows[27]:

$$E_0 = \sum_{j=1}^{v} \varepsilon_j - \frac{1}{2}\int \frac{n(r)n(r')}{|r-r'|}drdr' - \int v_{xc}(r)n(r)dr + E_{xc}[n(r)] \quad (15)$$

Here, the ε_j and $n(r)$ are self consistent quantities.

For this theory to be practically useful, we require a good approximation to $E_{xc}[n(r)]$. To serve this purpose, a local density approximation (LDA) is used[28]:

$$E_{xc}^{LDA}[n(r)] = \int e_{xc}(n(r))n(r)dr \quad (16)$$

Here $e_{xc}(n)$ is known as exchange –correlation energy per particle of a uniform interacting electron gas of density $n(r)$ which is obtained with a very high accuracy (~0.1%). In DFT the computing time is proportional to N_{atom}^2 or N_{atom}^3. However in traditional methods, computing time grows as $e^{\alpha N}$ where α is ~1. Hence, DFT has become a widely accepted and popular method to study large systems like macromolecules and clusters where $N_{atoms} \approx 100-200$,

making the cost of calculations computational viable and yet offering an extremely reasonable accuracy.

2.3. Exchange Correlation Functionals:

There are various kinds of exchange correlation functionals, which have been employed in computational chemistry. Some of the functionals are B3LYP[29-30], M05[31], M05-2X[31], M06-2X[32], etc. The applicability of the functional depends upon the system and the properties of interest. The M05-2X is a high non-locality functional with twice the amount of non-local exchange (2X) that is parameterized only for non-metals. It has been observed that M05-2X (which is hybrid meta exchange-correlation functional) has the best performance for non-covalent interactions like hydrogen bonding, pi---pi stacking and interaction energies of the nucleobases. We found this functional to be the most appropriate for the present work as clathrate hydrates have a large number of hydrogen bonding sites and dispersion interactions which can be well described by the M05-2X functional.

2.4. DFT application to chemical systems:

For any chemical system, Parr and co-workers[33] described the electronic chemical potential (μ) as:

$$\mu = \left(\frac{\partial E}{\partial N}\right)_v \tag{17}$$

Here E is the electronic energy, N is number of electrons, v is an external potential due to the nuclei. The chemical potential μ, is the instantaneous slope which can be determined using the method of finite differences. By using a finite difference approximation to eqn.17, the chemical potential is written as:

$$\mu = -\left[\frac{E(N+1) - E(N-1)}{2}\right] \text{ or } \mu \approx -\left(\frac{I+A}{2}\right) \tag{18}$$

Further,
$$\left(\frac{I+A}{2}\right) = \chi_m = -\mu \tag{19}$$

where, χ_m is known as Mulliken electronegativity. Since it has a fundamental relationship to the chemical potential, it is termed as absolute electro-negativity[33] (χ) which reflects the property of entire molecule, ion, or system. To understand the stability of any chemical system,

hardness is defined as the measure of the resistance to change in the electronic distribution in any chemical system. Parr and Pearson[34-35] defined chemical hardness:

$$\eta = \frac{1}{2}\left(\frac{\partial^2 E}{\partial N^2}\right)_v \quad \text{or} \quad \eta = \frac{1}{2}(I - A) \tag{20}$$

I and A are calculated using the Koopmans' theorem[24] and is defined as:

$$I = -E_{homo} \quad \text{and} \quad A = -E_{lumo}$$

The electro-philicity index[36] (ω) for a chemical system as:

$$\omega = \frac{\chi^2}{2\eta} \tag{21}$$

Here, ω describes the reactivity of the system. These reactivity indices have been used in previous ab *initio* calculations on clathrate hydrates[7, 21-22] and hence we have chosen these indices as one of the measurements of stability of clathrate hydrates in our present work.

2.5. Computational details:

All calculations in this work were performed using the Gaussian 03[37] program. The initial cages (5^{12}, $5^{12}6^2$, and $5^{12}6^4$) were constructed based on the work of McMullan *et al.*[8].Each cage was further optimized using the 6-311++G** basis set. The obtained geometries of the individual cages were further re-optimized by varying the occupancies of different gases inside 5^{12}, $5^{12}6^2$ and $5^{12}6^4$ cages with the 6-311++G** basis set. The optimization was performed by using Berny algorithm[38] using a tight convergence criteria and a fine grid. Basis set superposition error (BSSE) using the counterpoise method[39-40], and frequency calculations were performed on the optimized structures.The total energies (E) obtained at the optimized geometry also includes corrections from BSSE and contributions from Zero Point Energy. The interaction energies (IE) which shows the stability of encapsulated gas molecules can be written as:

$$IE = E(\text{gas-cage}) - E(\text{cage}) - n*E(\text{gas}) \tag{22}$$

Here, n is the number of gas molecules, E (gas) is the total energy of a free gas molecule. E (cage) is the total energy of the gas free water cages. E (gas-cage) is the total energy of the encapsulated gas molecule(s) in a particular cage.

3. Results and Discussion:

3.1. H_2 encapsulation:

3.1.1. Structural Properties:

The structural parameters with varying occupancies of H_2 in 5^{12}, $5^{12}6^2$ and $5^{12}6^4$ cages are shown in Table 2. An examination of cavity radii with varying occupancies of H_2 (structures shown in Fig. 2) shows the following features: The radius of the cage increase with all occupancies of H_2 relative to the 5^{12} cage. For *e.g.*; a single occupancy of the H_2 molecule in the 5^{12} cage increase the cavity radii by 6 %. The double occupancy of H_2 molecules increases the cavity radii by 8 %. Such a large increase in the cavity radii is because the two H_2 molecules maintain an average distance of 2.80 Å. The triple occupancy of H_2 molecules increases the cavity radii by 9 %. The triple occupancy shows a triangular arrangement of H_2 molecules with an average distance of 2.38 Å (as seen in Fig 2c). A structural deformation occurs with the quadruple occupancy of H_2 molecules.

Table 2: Average bond length and angle with varying occupancy of H_2 in 5^{12}, $5^{12}6^2$ and $5^{12}6^4$ cages. Deviation in parenthesis.

Structure	Cavity radii (Å)	$O_W \cdots O_W$ (Å)	$H_W \cdots O_W$ (Å)	$O_W \cdots O_W \cdots O_W$ (deg)
5^{12}	3.72	2.76 (0.12)	1.84 (0.10)	107.70 (3.1)
$5^{12}(H_2)$	3.94	2.77 (0.11)	1.80 (0.12)	107.35 (5.9)
$5^{12}(H_2)_2$	4.04	2.71 (0.13)	1.80 (0.13)	107.55 (6.1)
$5^{12}(H_2)_3$	4.05	2.80 (0.13)	1.83 (0.11)	107.73 (5.5)
$5^{12}6^2$	4.63	2.71 (0.10)	1.74 (0.12)	113.10 (5.9)
$5^{12}6^2(H_2)$	4.42	2.70 (0.11)	1.73 (0.12)	113.91 (6.8)
$5^{12}6^2(H_2)_2$	4.48	2.76 (0.10)	1.70 (0.13)	113.87 (7.2)
$5^{12}6^2(H_2)_3$	4.53	2.74 (0.10)	1.73 (0.16)	113.98 (7.0)
$5^{12}6^4$	4.57	2.75 (0.11)	1.77 (0.12)	113.28 (5.6)
$5^{12}6^4(H_2)$	4.51	2.75(0.10)	1.77 (0.13)	113.19 (7.0)
$5^{12}6^4(H_2)_2$	4.57	2.77 (0.11)	1.78 (0.11)	112.17 (8.1)
$5^{12}6^4(H_2)_3$	4.66	2.77 (0.11)	1.80 (0.11)	112.99 (6.4)
$5^{12}6^4(H_2)_4$	4.71	2.71 (0.21)	1.74 (0.12)	113.83 (5.6)
$5^{12}6^4(H_2)_5$	4.78	2.78 (0.12)	1.85 (0.10)	112.62 (7.9)

The average $O_W \cdots O_W$ distance from a single occupancy in the 5^{12} cage is 2.77 Å. The average $H_W \cdots O_W$ distance is 1.80 Å. The $O_W \cdots O_W \cdots O_W$ angle varies from 102.76° to 119.15°. The structural features of single occupancy are in agreement with the results of Satyamurthy and co-workers[7] in which the authors showed that the encapsulation of the guest species does not distort the cage significantly. The $O_W \cdots O_W$ distance for double occupancies varies from 2.62 Å to 2.94 Å. The $H_W \cdots O_W$ distance varies from 1.52 Å to 2.00 Å. The $O_W \cdots O_W \cdots O_W$ angle varies from 102.17° to 119.16°. The $O_W \cdots O_W$ distance for the triple occupancies inside the 5^{12} cage varies from 2.52 Å to 3 Å. The $H_W \cdots O_W$ distance varies from 1.61 Å to 1.97 Å. The $O_W \cdots O_W \cdots O_W$ angle varies from 102.03° to 114.17°. Thus the structural integrity of the cages remains intact with varying occupancies of H_2.

In the $5^{12}6^2$ cage, we find stationary points of inclusion for a triple occupancy of H_2 with no imaginary frequencies. However, two negative frequencies are observed with a quadruple occupancy. An examination of cavity radii with varying occupancies of gases shows a decrease in the cavity radii. The single occupancy shows a contraction of the cage. The double occupancy shows an average distance between the two H_2 molecules of about 2.89 Å. The triple occupancy shows a triangular arrangement among the H_2 molecules separated at a average distance of 2.47 Å. The structural features for varying occupancies of H_2 molecules in the $5^{12}6^2$ are cages similar to 5^{12} cage. The $O_W \cdots O_W$ distance for all occupancies of H_2 molecules varies from 2.70 Å - 2.76 Å. Only slight deviations are observed for double and triple occupancies. Similar trends are also observed in the $H_W \cdots O_W$ distance and $O_W \cdots O_W \cdots O_W$ angle.

In the $5^{12}6^4$ cage, quintuple occupancy of H_2 molecules is observed. Similar to the $5^{12}6^2$ cage, a slight decrease in the cavity radii is observed on a single occupancy of H_2 in the $5^{12}6^4$ cage. A double occupancy shows two H_2 molecules a distance of 2.89 Å. The triple occupancy shows that H_2 molecules also show a triangular arrangement with a average distance of 2.48 Å. An average distance of 2.8 Å is seen for quadruple and quintuple occupancies of H_2. A structural deformation of the cage occurs with the encapsulation of six H_2 molecules. The

structural features for varying occupancies inside the $5^{12}6^4$ cage also shows similar features like other cages. For e.g.; the $O_W \cdots O_W$ distance for all occupancies of H_2 molecules inside the $5^{12}6^4$ cages is 2.71 Å - 2.78 Å. Only slight deviations are observed for quadruple occupancies.

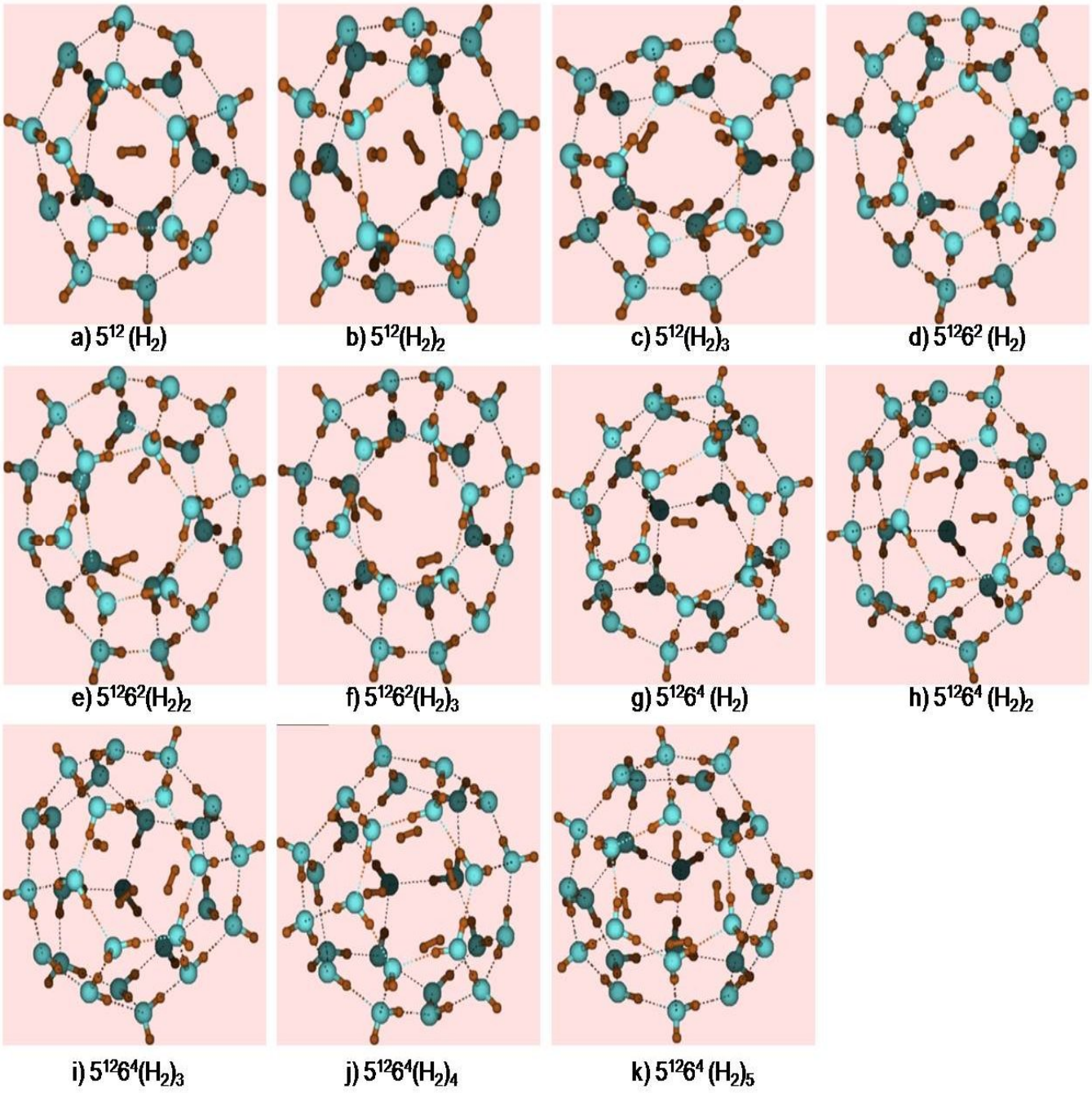

Figure 2: Encapsulation of H_2 molecules inside the 5^{12}, $5^{12}6^2$ and $5^{12}6^4$ cages.

3.1.2. Interaction energies:

The interaction energy (IE) for all H_2 occupancies in 5^{12}, $5^{12}6^2$ and $5^{12}6^4$ cages are shown in Table 3. The IE calculations show that a triple occupancy offers maximum stability to the 5^{12} cage. The IE energies shows that the triple occupancy is slightly more stable compared to the double occupancy. However, both the double and triple occupancy are extremely stable compared to the single occupancy. A comparison of IE values from our work shows the single occupancy is more stabilized by 4.66 kcal/mol compared to the results of Satyamurthy and co-workers[7] on 5^{12} cages. The difference arises due to the choice of method and basis set used in our work. Chattaraj *et al.*[21] showed that a maximum stability is achieved for the double occupancies in the 5^{12} and $5^{12}6^2$ cages. The IE in the 5^{12} cage from our work for double and triple occupancies is more stabilized by 4.26 kcal/mol and 5.9 kcal/mol compared to the results of Chattaraj *et al*.[21] This difference is because the work of Chattaraj *et al*.[21] uses the B3LYP functional which lacks description of dispersion which is important in these cages. Similar to the 5^{12} cage, the triple occupancies are more stable than single and double occupancies in the $5^{12}6^2$ cage. In the $5^{12}6^4$ cage, maximum stability is seen from the quadruple occupancy of H_2 molecules. Chattaraj *et al.*[21] observed that for $5^{12}6^4$ cage, minimum energy structures are not found and their efforts to minimize structures lead to structural deformation. Further, the authors also neglected corrections from BSSE and ZPE correction which is significant to the calculation of interaction energies.

3.1.3. Reactivity descriptors:

The η of single occupancy is 9.277 eV. Upon the encapsulation of the H_2 molecule, η increases, which show an increase in rigidity (i.e. increase in the resistance to change in the electron distribution in any chemical system). The reactivity descriptors calculated for varying occupancies in the $5^{12}6^2$ cage also shows trends similar to the 5^{12} cage. The electro-philicity (ω) decreases as the number of H_2 molecules increased inside the $5^{12}6^2$ cage. In the case of the $5^{12}6^4$ cage, the stability of $5^{12}6^2$ cavity also increases with increasing occupancy of H_2. For each cage, the maximum η is consistent with the maximum stability seen from the IE values.

Table 3: Total energy, Interaction energy (IE), Electro-negativity (χ), Hardness (η), and Electro-philicity (ω) with varying occupancy of H_2 in 5^{12}, $5^{12}6^2$ and $5^{12}6^4$ cages.

Structure	E(a.u.)	IE(kcal/mol)	χ(eV)	η(eV)	ω(eV)
$5^{12}(H_2)$	-1529.7988	-7.02	4.657	9.277	1.169
$5^{12}(H_2)_2$	-1530.9563	-10.67	4.678	9.374	1.167
$5^{12}(H_2)_3$	-1532.1063	-10.84	4.691	9.452	1.164
$5^{12}6^2(H_2)$	-1835.5458	-6.25	5.303	10.032	1.400
$5^{12}6^2(H_2)_2$	-1836.7046	-11.51	4.983	10.591	1.172
$5^{12}6^2(H_2)_3$	-1837.8596	-14.71	4.995	10.708	1.165
$5^{12}6^4(H_2)$	-2142.0568	-5.53	4.876	9.739	1.221
$5^{12}6^4(H_2)_2$	-2143.2273	-16.80	4.821	9.789	1.429
$5^{12}6^4(H_2)_3$	-2144.3975	-25.06	4.849	9.805	1.199
$5^{12}6^4(H_2)_4$	-2145.5326	-31.02	4.790	9.705	1.182
$5^{12}6^4(H_2)_5$	-2146.5881	2.84	3.840	7.812	0.944

3.2. O_2 encapsulation:

3.2.1. Structural Properties:

The structural parameters with varying occupancies of O_2 in 5^{12}, $5^{12}6^2$ and $5^{12}6^4$ cages are shown in Table 4. An examination of cavity radii with varying occupancies of O_2 (structures shown in Fig. 3) shows the following features: The radius of the cage increase with all occupancies of O_2 relative to the 5^{12} cage. For *e.g.*; a single occupancy of the O_2 molecule in the 5^{12} cage increase the cavity radii by 7.5 %. The double occupancy of O_2 molecules increases the cavity radii by 13 %. Such a large increase in the cavity radii is because the two O_2 molecules maintain an average distance of 1.65 Å. Further encapsulation of O_2 molecules lead to the disintegration of the cage structure. The average $O_W \cdots O_W$ distance in a single occupancy is 2.85 Å. In double occupancy, the average $O_W \cdots O_W$ distance is 3 Å. The deviation in the $O_W \cdots O_W$ distance is found to be large for double occupancies compared to single occupancy. Similar trends are observed for the $H_W \cdots O_W$ distance and $O_W \cdots O_W \cdots O_W$ angle. In the $5^{12}6^2$ cage, the cavity radii increase with increasing occupancy of O_2 molecules (as seen in Table 4). For a double occupancy in the $5^{12}6^2$ cage, the two O_2 molecules maintain a distance 1.45 Å, whereas for a triple occupancy in the $5^{12}6^2$ cage, the three O_2 molecules

maintain an average distance of 2.7 Å. An encapsulation of a fourth O_2 molecule shows a structural deformation of the cage. The average $O_W \cdots O_W$ distance for varying occupancies of O_2 is 2.75 Å. The deviation in the $O_W \cdots O_W$ distance is found to be similar for all occupancies.

Table 4: Average bond length and angle with varying occupancy of O_2 in 5^{12}, $5^{12}6^2$ and $5^{12}6^4$ cages. Deviation in parenthesis.

Structure	Cavity radii (Å)	$O_W \cdots O_W$ (Å)	$H_W \cdots O_W$ (Å)	$O_W \cdots O_W \cdots O_W$ (deg)
$5^{12}(O_2)$	4.00	2.85 (0.06)	1.88 (0.06)	109.44 (3.5)
$5^{12}(O_2)_2$	4.20	3.00 (0.03)	2.05 (0.02)	107.97 (2.2)
$5^{12}6^2(O_2)$	4.49	2.77 (0.10)	1.87 (0.16)	109. 34 (7.4)
$5^{12}6^2(O_2)_2$	4.50	2.75 (0.10)	1.76 (0.11)	115.27 (5.1)
$5^{12}6^2(O_2)_3$	4.56	2.74 (0.10)	1.77 (0.11)	110.20 (6.8)
$5^{12}6^4(O_2)$	4.58	2.75 (0.10)	1.79 (0.11)	113.02 (7.0)
$5^{12}6^4(O_2)_2$	4.60	2.75 (0.11)	1.78 (0.12)	113.01 (7.8)
$5^{12}6^4(O_2)_3$	4.65	2.77 (0.10)	1.79 (0.12)	112.98 (6.9)
$5^{12}6^4(O_2)_4$	4.70	2.77 (0.11)	1.79 (0.12)	112.35 (7.1)

In the $5^{12}6^4$ cage, minimum energy structures were found up-to quadruple occupancy. The radius of cavity increases with the encapsulation of O_2 in the $5^{12}6^4$ cage (as shown in Table 4). For a double occupancy, the two O_2 molecules maintain a distance 1.45 Å, whereas a triple occupancy, the three O_2 molecules maintain an average distance of 2.79 Å. For quadruple occupancy, the average distance is 3 Å. Further encapsulation leads to a structural deformation of the cage.

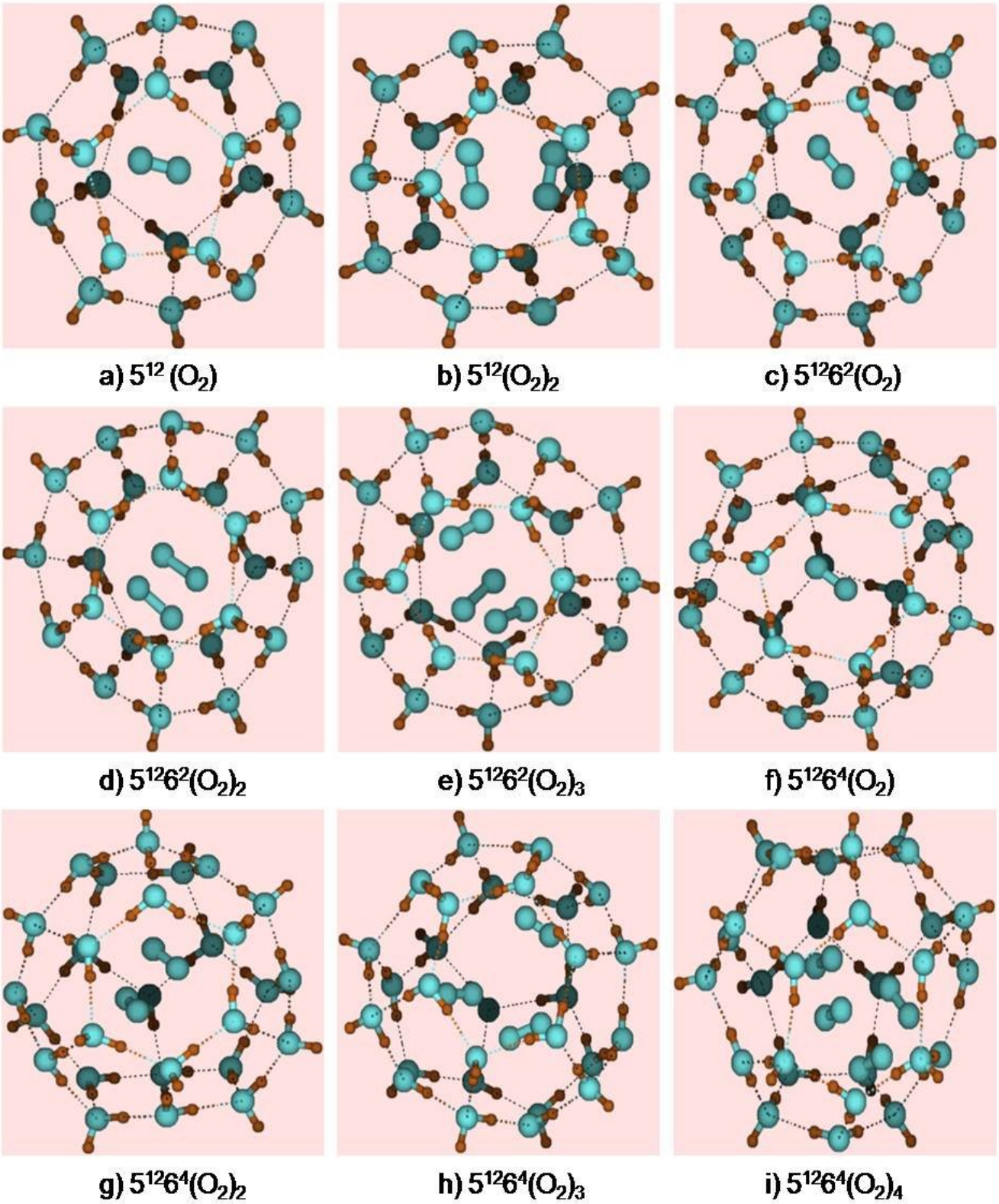

Figure 3: Encapsulation of varying O_2 molecules inside the 5^{12}, $5^{12}6^2$ and $5^{12}6^4$ cages.

3.2.2. Interaction energies:

The IE for varying occupancies is shown in Table 5. An examination of IE shows that the double occupancy is more stable compared to the single occupancy of the 5^{12} cage. Similarly for the $5^{12}6^2$ cage, the triple occupancies are more stable compared to single and double occupancies. For the $5^{12}6^4$ cage, the double occupancy is the most stable, though triple and quadruple occupancy does not show any structural deformation. The positive IE values of triple and quadruple occupancies suggest that they can be easily destabilized.

3.2.3. Reactivity descriptors:

Table 5 shows the reactivity descriptors for the varying uptake of O_2 molecules in 5^{12}, $5^{12}6^2$, and $5^{12}6^4$ cages. In 5^{12} and $5^{12}6^2$ cages, we could not find any direct correlation of the reactivity indices with the IE values and hence this requires a more in-depth investigation. However, in the $5^{12}6^4$ cage, η is found to be a maximum for the double occupancy and is consistent with the maximum stability seen from the IE.

Table 5: Total energy, Interaction energy (IE), Electro-negativity (χ), Hardness (η), and Electro-philicity (ω) with varying occupancy of O_2 in 5^{12}, $5^{12}6^2$ and $5^{12}6^4$ cages.

Structure	E(a.u.)	IE(kcal/mol)	χ(eV)	η(eV)	ω(eV)
$5^{12}(O_2)$	-1678.9187	-7.87	5.962	6.162	2.884
$5^{12}(O_2)_2$	-1829.1901	-10.84	6.267	5.149	3.814
$5^{12}6^2(O_2)$	-1984.6650	-6.43	5.013	10.709	1.184
$5^{12}6^2(O_2)_2$	-2134.8814	-12.44	4.973	10.580	1.169
$5^{12}6^2(O_2)_3$	-2285.1567	-15.62	5.790	8.828	1.899
$5^{12}6^4(O_2)$	-2291.1692	-3.79	5.696	6.165	2.632
$5^{12}6^4(O_2)_2$	-2488.2415	-6.80	5.789	7.187	1.189
$5^{12}6^4(O_2)_3$	-2591.5630	6.82	4.095	4.244	1.976
$5^{12}6^2(O_2)_4$	-2741.6503	15.91	5.509	3.102	4.892

3.3. N_2 encapsulation:

3.3.1 Structural Parameters:

The structural parameters with varying occupancies of N_2 in 5^{12}, $5^{12}6^2$ and $5^{12}6^4$ cages are shown in Table 6. An examination of cavity radii with varying occupancies of N_2 (structures shown in Fig. 4) shows the following features: The radius of the cage increase with all occupancies of N_2 relative to the 5^{12} cage. For *e.g.*; a single occupancy of the N_2 molecule in the 5^{12} cage increase the cavity radii by 4.8 %. The double occupancy of N_2 molecules increases the cavity radii by 13 %. The average $O_W \cdots O_W$ distance for the single occupancy is 2.78 Å whereas; the average $H_W \cdots O_W$ distance is 1.83 Å. The average $O_W \cdots O_W \cdots O_W$ angle is 107.49°. The average $O_W \cdots O_W$ distance for the double occupancy is 2.80 Å whereas; the average $H_W \cdots O_W$ distance is 1.85 Å. The minimum energy structures were found to be only up to triple occupancy in the $5^{12}6^2$ cage.

Table 6: Average bond length and angle with varying occupancy of N_2 in 5^{12}, $5^{12}6^2$ and $5^{12}6^4$ cages. Deviations are in parenthesis.

Structure	Cavity radii (Å)	$O_W \cdots O_W$ (Å)	$H_W \cdots O_W$ (Å)	$O_W \cdots O_W \cdots O_W$ (deg)
$5^{12}(N_2)$	3.90	2.78 (0.12)	1.83 (0.10)	107.49 (6.9)
$5^{12}(N_2)_2$	4.16	2.80 (0.17)	1.85 (0.13)	105.31 (5.5)
$5^{12}6^2(N_2)$	4.44	2.74 (0.10)	1.74 (0.11)	111.72 (8.4)
$5^{12}6^2(N_2)_2$	4.53	2.78 (0.10)	1.80 (0.10)	113.42 (8.6)
$5^{12}6^2(N_2)_3$	4.69	2.72 (0.10)	1.75 (0.10)	113.32 (8.1)
$5^{12}6^4(N_2)$	4.62	2.78 (0.10)	1.79 (0.10)	112.43 (8.1)
$5^{12}6^4(N_2)_2$	4.65	2.75 (0.11)	1.77 (0.13)	113.10 (6.6)
$5^{12}6^4(N_2)_3$	4.68	2.78 (0.12)	1.82 (0.13)	112.53 (5.9)
$5^{12}6^4(N_2)_4$	4.71	2.76 (0.10)	1.79 (0.11)	112. 48 (7.5)

For the double occupancy of the $5^{12}6^2$ cage, the two N_2 molecules maintain an average distance of 3.47 Å. In the case of triple occupancy of the $5^{12}6^2$ cage we find a unusual arrangement of three N_2 molecules as seen in Fig 4e. We have repeated these calculations with varying input geometries of the three N_2 molecules (keeping the same input cage

structure) and we obtain the same final configuration and energy. The structural parameters for the different initial inputs, intermediates, and the final geometries are shown in Table 7. The structural properties for all structures show similar features. In the case of fourth N_2 molecule, the minimum energy structure is not obtained which leads to the structural deformation. In the $5^{12}6^4$ cage, a quadruple occupancy was achieved without any structural deformation of the cage.

Table 7: Average bond length and angle of $5^{12}6^2(N_2)_3$ uptake with different inputs

Structure	Cavity radii (Å)	$O_W \cdots O_W$ (Å)	$H_W \cdots O_W$ (Å)	$O_W \cdots O_W \cdots O_W$ (°)
a	4.48	2.61-2.88	1.61-1.91	96.35- 121.72
b	4.49	2.57-2.87	1.55-1.90	97.95- 124.06
c	4.49	2.61-2.87	1.62-1.91	98.86- 123.20
d	4.53	2.56-2.85	1.54-1.88	104.55-130.38
a'	4.56	2.61-2.90	1.62-1.93	100.52-121.58
b'	4.44	2.61-2.87	1.61-1.91	100.12-119.82
c'	4.47	2.53-2.87	1.57-1.89	101.39-122.36
d'	4.53	2.64-2.86	1.66-1.88	98.17- 130.31
a"	4.58	2.53-2.89	1.58-1.92	101.72- 121.96
b"	4.46	2.48-2.72	1.52-1.80	99.87 - 123.69
c"	4.47	2.63-2.84	1.61-1.86	103.67- 121.62
d"	4.53	2.65-2.84	1.65-1.89	99.17 - 123.31

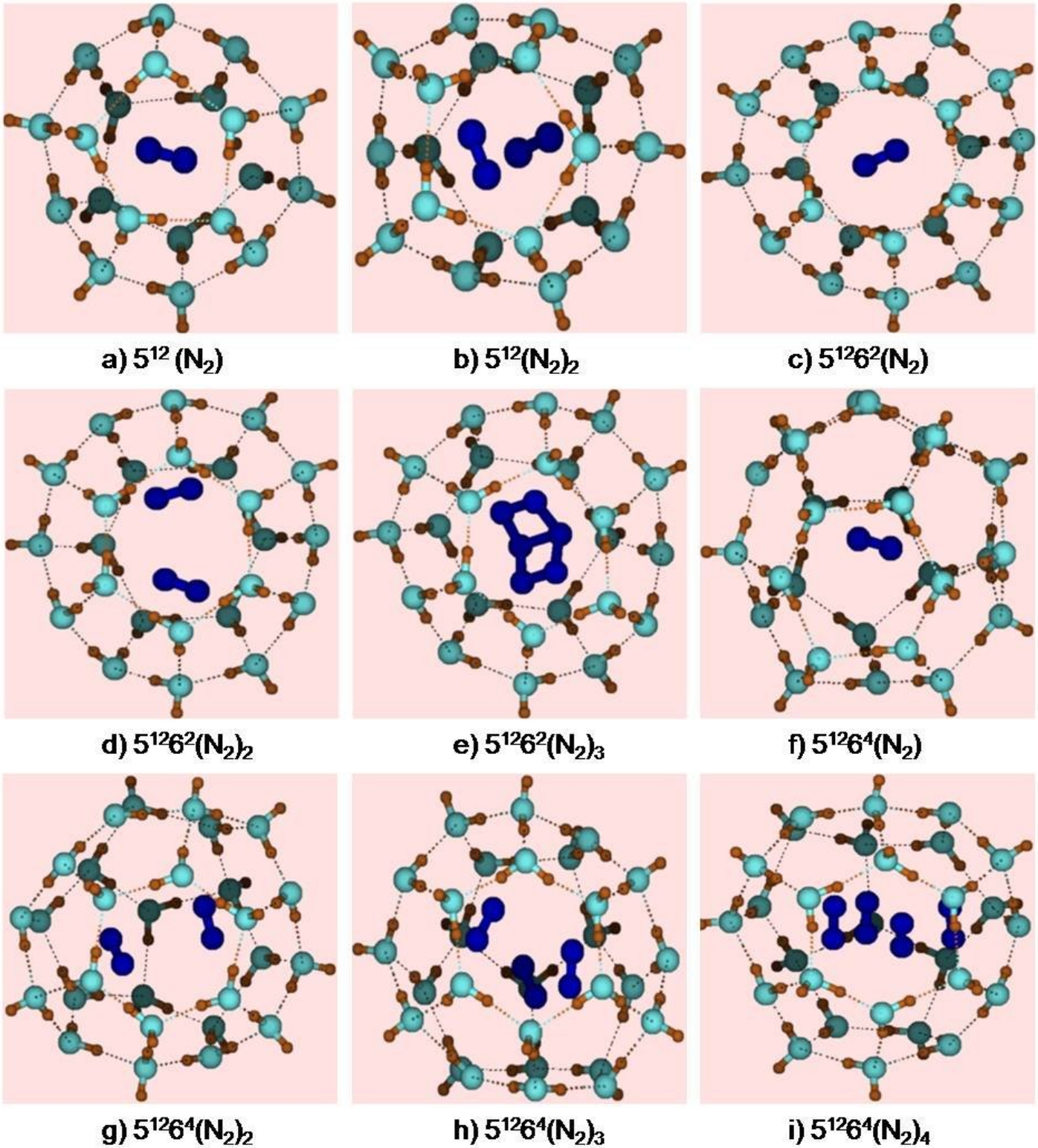

Figure 4: Encapsulation of varying N_2 molecules inside the 5^{12}, $5^{12}6^2$ and $5^{12}6^4$ cage

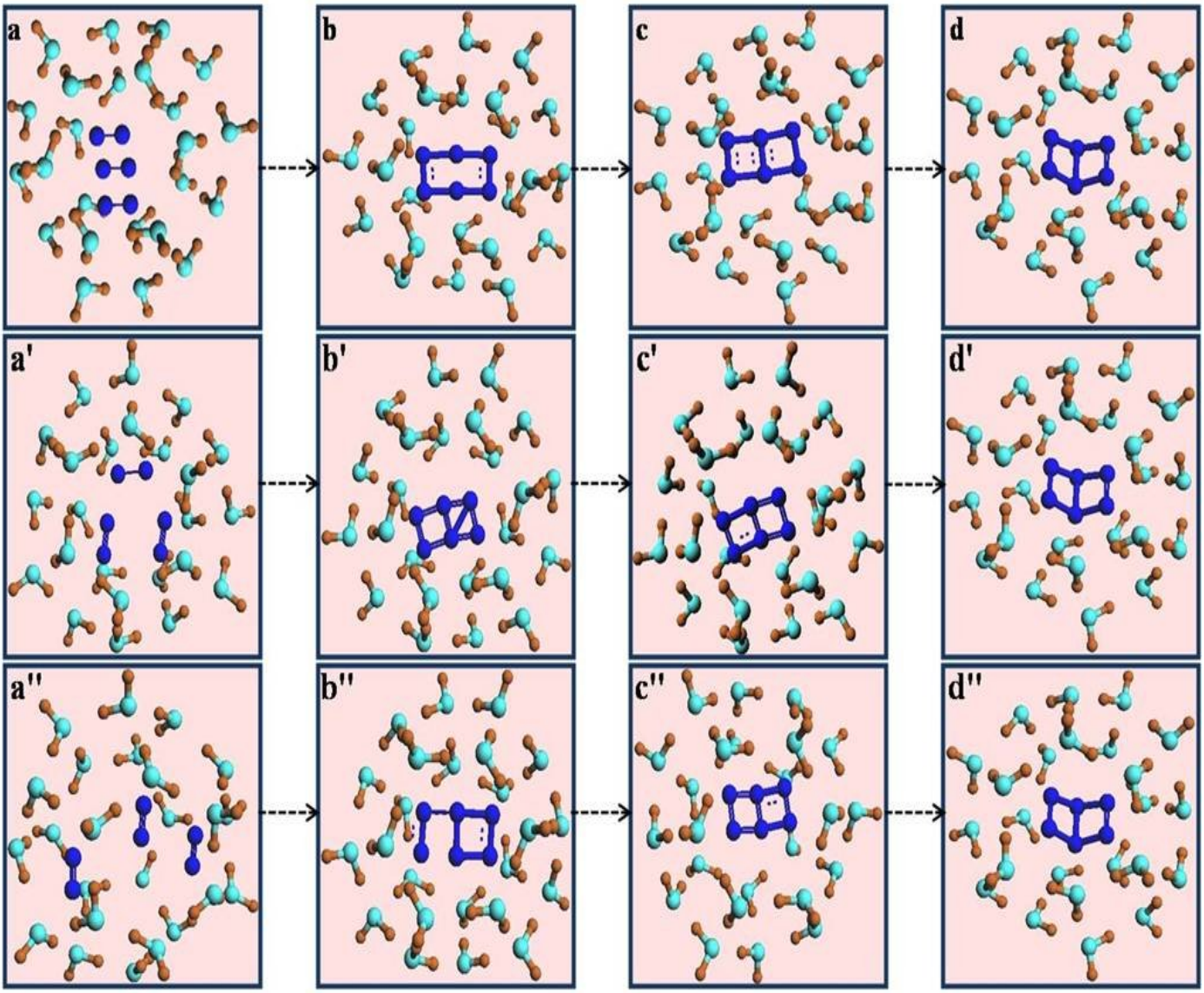

Figure 5: Optimization of $5^{12}6^2(N_2)_3$ cage with varying input configurations of N_2 molecules.

3.3.2. Interaction Energies:

The IE values for the varying occupancy of N_2 in 5^{12}, $5^{12}6^2$ and $5^{12}6^4$ cages are shown in Table 8. The IE for double occupancies in 5^{12} cage is more stable compared to single occupancy. In the $5^{12}6^2$ cage, the single occupancy is more stable compared to double and triple occupancies. The IE for triple occupancies in the $5^{12}6^4$ cage is more stable compared to single, double and quadruple occupancies.

Table 8: Total energy, Interaction energy (IE), Electro-negativity (χ), Hardness (η), and Electro-philicity (ω) with varying occupancy of N_2 in 5^{12}, $5^{12}6^2$ and $5^{12}6^4$ cages.

Structure	E(a.u.)	IE(kcal/mol)	χ(eV)	η(eV)	ω(eV)
$5^{12}(N_2)$	-1638.1863	-6.13	4.662	9.314	1.167
$5^{12}(N_2)_2$	-1748.2887	-8.44	4.707	9.547	1.160
$5^{12}6^2(N_2)$	-1943.9326	-4.59	5.695	6.180	2.624
$5^{12}6^2(N_2)_2$	-2053.4675	-3.80	5.798	5.984	2.808
$5^{12}6^2(N_2)_3$	-2162.6271	-2.83	5.593	6.212	2.517
$5^{12}6^4(N_2)$	-2250.4388	-6.64	4.882	9.748	1.222
$5^{12}6^4(N_2)_2$	-2359.9938	-7.47	4.879	9.862	1.207
$5^{12}6^4(N_2)_3$	-2469.5441	-8.93	4.878	9.900	1.202
$5^{12}6^2(N_2)_4$	-2577.5144	1.09	4.315	4.590	2.028

3.3.3. Reactivity descriptors:

We observe that η increases (ω decreases) on the double occupancy of N_2 in the 5^{12} cage. This suggests that the double occupancy is the most stable in the 5^{12} cage and these results are also consistent with IE. In the $5^{12}6^2$ cage, we could not find any direct correlation between the changes in reactivity indices with IE, though the single occupancy shows more hardness compared to double occupancy. However, in the $5^{12}6^4$cage, η is maximum for triple occupancy which is also consistent with IE.

4. Concluding Remarks:

We have characterized the structure and stability with varying occupancies of H_2, N_2, and O_2 in various cages of sI and sII hydrates using the DFT method. The stability of these gases is seen from the following trends: (**a)** Among the single and double occupancies in the 5^{12} cage, the order of stability is $O_2 > H_2 > N_2$. Compared to other occupancies, a triple occupancy of H_2 and a double occupancy of O_2 and N_2 show maximum stability in the 5^{12} cage. (**b)** Among the single, double and triple occupancies in the $5^{12}6^2$ cage, the order of stability is $O_2 > H_2 > N_2$. Compared to other occupancies, a triple occupancy of H_2 and O_2 and a single occupancy of N_2 show a maximum stability in the $5^{12}6^2$ cage. (**c)** Among the double, triple and quadruple occupancies in the $5^{12}6^4$ cage, the order of stability is $H_2 > N_2 > O_2$. However, for a single occupancy in the $5^{12}6^4$ cage, the order of stability is $N_2 > H_2 > O_2$. Compared to other occupancies, a quadruple occupancy of H_2, a double occupancy of O_2 and a triple occupancy of N_2 show maximum stability in the $5^{12}6^4$ cage.

The stability of the encapsulated clathrate hydrates has also been understood from the reactivity descriptors. The hardness (η) increases with the increasing number of H_2 molecules which leads to the decrease in the electrophilicity (ω). Similar trends are observed for the N_2 clathrate hydrates but there are some discrepancies observed for the O_2 clathrate hydrates. Hence, the reactivity descriptors indicate that an increasing number of H_2 as well as for N_2 molecules inside the different water cages leads to the stability of these clathrate hydrates which is seen from the hardness (η) as well as electrophilicity (ω). The triple occupancy of N_2 molecules inside the $5^{12}6^2$ cage follows an unusual geometry. Hence from the interaction energies and the DFT based reactivity descriptors indicate that stability of the clathrate hydrates increases with the increase in the number of gas molecules in most cases. The *ab initio* calculations presented in this work provides an excellent benchmark for capture and storage of these di atomic gases in sI and sII hydrate lattice. The level of theory and the quality of basis set employed may influence the trapping ability of a clathrate hydrates.

5. References:

1. Boswell, R. *Science* **2009**, *325*, 957-958
2. Sloan, E. D.; Koh, C. A. Clathrate Hydrates of Natural Gases, 3rd ed. CRC, Boca Raton, FL, **2007**.
3. Sloan, E. D. *Nature* **2003**, *426*, 353-359.
4. Sum, K.; Koh, C. A.; Sloan, E. D. *Ind Eng Chem Res* **2009**, *48*, 7457-7465.
5. Kvenvolden, K. A. Gas hydrate and humans, *Ann NY Acad Sci* **2000**, *912*, 17-22.
6. Nath, K. *J. Surface. Sci. Technol.* **2007**, *23*, 59-72.
7. Kumar, P.; Satyamurthy, N. *J. Phys. Chem. A.* **2011**, *115*, 14276-14281.
8. McMullan, R. K.; Jeffrey, G. A. *J. Chem. Phys.* **1965,** *42,* 2725-2732.
9. Sloan, E. D. *Nature* **2003**, *426*, 353-359.
10. Jacobsan, C. L.; Hujo, W.; Molinero, V. *J.Phys.Chem.B* **2010***, 114,* 13796-13807.
11. Moon, C.; Taylor, C.P.; Rodger, M. P. *Can. J.Phys.***2003***, 81,* 451-457.
12. Moon, C.; Taylor, C.P.; Rodger, M.P.; *J. Am. Chem. Soc.* **2003**, *125*, 4706-4707.
13. Hawtin, R. W.; Quigley, D.; Rodger, P. M. *Phys. Chem. Chem. Phys.* **2008**, *10*, 4853-4864.
14. Sun, Q.; Duan, Ti-Yu.; Zheng, H. F.; Jian, Q. J. *J. Chem. Phys.* **2005***, 122,* 024714-024717.
15. Sum, K.A.; Buruss, C. R.; Sloan, D. E. *J. Phys. Chem.* ***1997****, 101,* 7371-7377.
16. Hester, C. K.; Dunk, M. R.; White, N., S.; Brewer, G.P.; Peltzer, T.E.; Sloan, D. E. *Geochim. Cosmochim. Acta****.2007****, 71,* 2947-2959
17. Horikawa, S.; Itoh, H.; Tabata, K.; Kawamura, K.; Hondoh, T. *J. Phys. Chem. B.* **1997,** *101,* 6290-6292.
18. VanKlaveren, E. P.; Michels, J. P. J.; Schouten, J. A.; Klug, D. D.; Tse, J. S. *J. Chem. Phys.* **2001,** *114,* 5745-5754.
19. Alavi, S.; Ripmeester, J. A.; Klug, D. D. *J. Chem. Phys.* **2005,** *123,* 024507-024514.
20. Patchkovskii, S.; Tse, J. S. Proc. Natl. Acad. Sci **2003**, *100,* 14645-14650.
21. Chattaraj, P. K.; Bandaru, S.; Mondal, S. *J. Phys. Chem. A* **2011,** *115,* 187-193.
22. Srivastava K. H.; Sastry.N.G. *J. Phys. Chem. A.***2011***, 115,* 7633-7637.
23. Lynch, B. J.; Truhlar, D.G. *J.Phys.Chem. A* **2003***, 107,* 8996-8999.
24. Szabo, A.; Ostlund S. N. Modern Quantum Chemistry, Dover Publications, Inc. ***1996.***
25. Kohn, W.; Becke, D. A., Parr.G.R. *J.Phys.Chem****.*****1996***, 100,* 12974-12980*.*
26. Hohenberg, P.; Kohn, W. *Phys.Rev.* **1964***,136,* B864-B871.

27. Kohn, W.; Sham, J.L. Phys. Rev. **1965**, *140,* A1133-A1138.
28. Kohn, W.; Becke, D.A.; Parr, G. R. *J.Phys.Chem.* **1996**, *100*, 12974-12980
29. Becke, A.D. Density-Functional thermochemistry III.The role of exact exchange. *J.Chem.Phys.***1993***, 98,* 5648-5652*.*
30. Becke, A.D. Density-functional exchange-energy approximation with correct asymptotic-behavior, *Phys.Rev.A* **1998***, 38,* 3098-3100*.*
31. Zhao, Y.;Truhlar, D.G. *J.Chem.Theory Comput.* **2006**, *2,* 364-382*.*
32. Zhao, Y.;Truhlar, D.G. *Theo. Chem. Acc.* **2008**, *41*, 157-167.
33. Parr, R.G.; Donnelly, R.A.; Levy, M.; Palke, W.E*. J.Chem.Phys.***1978**, *68,* 3801-3807.
34. Parr, R.G.; Pearson, R.G. *J. Am.Chem. Soc.* **1983***, 105,* 7512-7516
35. Parr, R.G and Yang W. Density Functional theory for atoms and molecules; Oxford University press: New York, **1989**.
36. Chattaraj, P.K.; Roy, D.R. *Chem.Rev.***2007***, 107,* PR46-PR74.
37. Frisch, M. J.; Trucks, G. W.; Schlegel, H. B.; Scuseria, G. E.; Robb,M. A.; Cheeseman, J. R.; Montgomery, J. A., Jr.; Vreven, T.; Kudin, K. N.;Burant, J. C.; Millam, J. M.; Iyengar, S. S.; Tomasi, J.; Barone, V.; Mennucci, B.; Cossi, M.; Scalmani, G.; Rega, N.; Petersson, G. A.; Nakatsuji, H.; Hada, M.; Ehara, M.; Toyota, K.; Fukuda, R.; Hasegawa, J.; Ishida, M.; Nakajima, T.; Honda, Y.; Kitao, O.; Nakai, H.; Klene, M.; Li, X.; Knox, J. E.; Hratchian, H. P.; Cross, J. B.; Bakken, V.; Adamo, C.; Jaramillo, J.; Gomperts, R.; Stratmann, R. E.; Yazyev, O.; Austin, A. J.; Cammi, R.; Pomelli, C.; Ochterski, J. W.; Ayala, P. Y.; Morokuma, K.; Voth, G. A.; Salvador, P.; Dannenberg, J. J.; Zakrzewski, V. G.; Dapprich, S.; Daniels, A. D.; Strain, M. C.; Farkas, O.; Malick, D. K.; Rabuck, A. D.; Raghavachari, K.; Foresman, J. B.; Ortiz, J. V.; Cui, Q.; Baboul, A. G.; Clifford, S.; Cioslowski, J.; Stefanov, B. B.; Liu, G.; Liashenko, A.; Piskorz, P.; Komaromi, I.; Martin, R. L.; Fox, D. J.; Keith, T.; Al-Laham, M. A.; Peng, C. Y.; Nanayakkara, A.; Challacombe, M.; Gill, P. M. W.; Johnson, B.; Chen, W.; Wong, M. W.; Gonzalez, C.; Pople, J. A. *Gaussian 03*, Revision B. 05; Gaussian, Inc.: Wallingford, CT, **2003**.
38. Peng, C.; Ayala, P. Y.; Schlegel, H. B.; Frisch, M. J. *J. Comp.Chem.* **1996**, *17*, 49-56.
39. Simon, S.; Duran, M.; Dannenberg, J. J. *J. Chem. Phys.* **1996***, 105,* 11024-11031.
40. Boys, S. F.; Bernardi, F. *Mol. Phys.* **1970***, 19,* 553-566.